

# PKS 2123–463: a confirmed $\gamma$ -ray blazar at high redshift

F. D’Ammando<sup>1,2,3\*</sup>, A. Rau<sup>4</sup>, P. Schady<sup>4</sup>, J. Finke<sup>5</sup>, M. Orienti<sup>6,3</sup>, J. Greiner<sup>4</sup>,  
D. A. Kann<sup>7</sup>, R. Ojha<sup>8,9</sup>, A. R. Foley<sup>10</sup>, J. Stevens<sup>11</sup>, J. M. Blanchard<sup>12</sup>,  
P. G. Edwards<sup>13</sup>, M. Kadler<sup>14,15</sup>, J. E. J. Lovell<sup>12</sup>

<sup>1</sup>*Dip. di Fisica, Università degli Studi di Perugia, Via A. Pascoli, I-06123 Perugia, Italy*

<sup>2</sup>*INFN - Sezione di Perugia, Via A. Pascoli, I-06123 Perugia, Italy*

<sup>3</sup>*INAF - Istituto di Radioastronomia, Via Gobetti 101, I-40129 Bologna, Italy*

<sup>4</sup>*Max-Planck-Institute für Extraterrestrische Physik, Giessenbachstraße 1, 85748 Garching, Germany*

<sup>5</sup>*U.S. Naval Research Laboratory, Code 7653, 4555 Overlook Ave. SW, Washington, DC 20375-5352, USA*

<sup>6</sup>*Dip. di Astronomia, Università di Bologna, Via Ranzani 1, I-40127 Bologna, Italy*

<sup>7</sup>*Thüringer Landessternwarte Tautenburg, Sternwarte 5, 07778 Tautenburg, Germany*

<sup>8</sup>*NASA, Goddard Space Flight Center, Greenbelt, MD 20771, USA*

<sup>9</sup>*IACS, Dept. of Physics, The Catholic University of America, 620 Michigan Ave., N.E., Washington, DC 20064, USA*

<sup>10</sup>*SKA SA, Cape Town Office 3rd Floor, The Park, Park Road, Pinelands, Cape Town, South Africa*

<sup>11</sup>*CSIRO Astronomy and Space Science, ATNF, Locked Bag 194, Narrabri NSW 2390, Australia*

<sup>12</sup>*School of Mathematics & Physics, Private Bag 37, University of Tasmania, Hobart TAS 7001, Australia*

<sup>13</sup>*CSIRO Astronomy and Space Science, ATNF, PO Box 76, Epping NSW 1710, Australia*

<sup>14</sup>*Institut für Theoretische Physik und Astrophysik, Universität Würzburg, 97074 Würzburg, Germany*

<sup>15</sup>*CRESST/NASA Goddard Space Flight Center, Greenbelt, MD 20771, USA*

Accepted. Received; in original form

## ABSTRACT

The flat spectrum radio quasar (FSRQ) PKS 2123–463 was associated in the First *Fermi*-LAT source catalog with the  $\gamma$ -ray source 1FGL J2126.1–4603, but when considering the full first two years of *Fermi* observations, no  $\gamma$ -ray source at a position consistent with this FSRQ was detected, and thus PKS 2123–463 was not reported in the Second *Fermi*-LAT source catalog. On 2011 December 14 a  $\gamma$ -ray source positionally consistent with PKS 2123–463 was detected in flaring activity by *Fermi*-LAT. This activity triggered radio-to-X-ray observations by the *Swift*, GROND, ATCA, Ceduna, and KAT-7 observatories. Results of the localization of the  $\gamma$ -ray source over 41 months of *Fermi*-LAT operation are reported here in conjunction with the results of the analysis of radio, optical, UV and X-ray data collected soon after the  $\gamma$ -ray flare. The strict spatial association with the lower energy counterpart together with a simultaneous increase of the activity in optical, UV, X-ray and  $\gamma$ -ray bands led to a firm identification of the  $\gamma$ -ray source with PKS 2123–463. A new photometric redshift has been estimated as  $z = 1.46 \pm 0.05$  using GROND and *Swift*/UVOT observations, in rough agreement with the disputed spectroscopic redshift of  $z = 1.67$ . We fit the broadband spectral energy distribution with a synchrotron/external Compton model. We find that a thermal disk component is necessary to explain the optical/UV emission detected by *Swift*/UVOT. This disk has a luminosity of  $\sim 1.8 \times 10^{46}$  erg s<sup>−1</sup>, and a fit to the disk emission assuming a Schwarzschild (i.e., nonrotating) black hole gives a mass of  $\sim 2 \times 10^9 M_{\odot}$ . This is the first black hole mass estimate for this source.

**Key words:** galaxies: active – galaxies: nuclei – quasars: general – quasars: individual (PKS 2123-463) – gamma rays

## 1 INTRODUCTION

Blazars constitute the most extreme subclass of Active Galactic Nuclei (AGN), characterized by the emission of

strong non-thermal radiation across the entire electromagnetic spectrum and in particular intense  $\gamma$ -ray emission above 100 MeV. The typical observational properties of blazars include irregular, rapid, high-amplitude variability, radio-core dominance, apparent super-luminal motion, a flat radio spectrum, and high and variable polarization at radio

\* E-mail: filippo.dammando@fisica.unipg.it

and optical frequencies. These features are interpreted as resulting from the emission of high-energy particles accelerated within a relativistic jet closely aligned with our line of sight and launched in the vicinity of the supermassive black hole harboured by the active galaxy (Blandford & Rees 1978; Urry & Padovani 1995).

Since the advent of the Energetic Gamma Ray Experiment Telescope (EGRET) on the Compton Gamma-Ray Observatory (CGRO), blazars were known to dominate the extragalactic high-energy sky. However, EGRET did not pinpoint the location of many sources with sufficient precision to enable astronomers to associate them with known objects, leaving the legacy of a large fraction of unidentified sources in  $\gamma$  rays. The point-spread function and sensitivity of the Large Area Telescope (LAT) on board *Fermi* provides an unprecedented angular resolution at high energies for localizing a large number of newly found  $\gamma$ -ray emitting sources. Correlated variability observed at different frequencies can give important information for the identification of a  $\gamma$ -ray source with its low-energy counterpart.

On 2011 December 14 a  $\gamma$ -ray flare from a source positionally consistent with PKS 2123–463 was detected by *Fermi*-LAT (Oriente & D’Ammando 2011), triggering GROND and *Swift* follow-up observations (Rau et al. 2011; D’Ammando et al. 2011) that confirmed contemporaneous activity in the optical/UV as well as marginally in X-rays.

PKS 2123–463 is a bright radio quasar with a luminosity at 1.4 GHz  $L_{1.4\text{GHz}} = (1.5 \pm 0.2) \times 10^{28}$  W/Hz (assuming the redshift estimated in this paper,  $z = 1.46 \pm 0.05^1$ ; see Sect. 6). On the basis of its spectral index  $\alpha_r \sim 0.4$  ( $S(\nu) \propto \nu^{-\alpha_r}$ ) between 408 MHz and 4.8 GHz, it was included in the CRATES catalog of flat spectrum objects (Healey et al. 2007). ATCA observations performed almost simultaneously at 4.8, 8.6 and 20 GHz during the Australia Telescope 20 GHz (AT20G) survey indicated a flattening of the radio spectrum at high frequencies to a spectral index of  $\alpha_r \sim 0.2$ . Polarized emission has been detected only at 4.8 GHz where the polarization is about 4% of the total intensity flux density (Massardi et al. 2008). A *Chandra* observation of PKS 2123–463 in March 2004 has shown the presence of a jet-like extended structure in X-rays (Marshall et al. 2011). The redshift of PKS 2123–463 was reported to be  $z = 1.67$  (Savage & Wright 1981) based on an objective-prism spectrum, subsequently questioned by Jackson et al. (2002) because two possible redshifts (0.48 and 1.67) were given from observation of two lines in the spectrum, and the motivation for the exclusion of the smaller redshift was not provided. This object was a member of the pre-*Fermi* launch Roma-BZCAT (Massaro et al. 2009) catalog listing candidate  $\gamma$ -ray blazars detectable by *Fermi*-LAT but not in the CGRaBS catalog (Healey et al. 2008).

The flat spectrum radio quasar (FSRQ) PKS 2123–463 (R.A.: 21h26m30.7042s, Dec.: –46d05m47.892s, J2000; Fey et al. 2006) was associated in the First *Fermi*-LAT source catalog (1FGL, 2008 August 4 – 2009 July 4; Abdo et al. 2010a) with the  $\gamma$ -ray source 1FGL J2126.1–4603, while no association with a  $\gamma$ -ray source was

present in the Second *Fermi*-LAT source catalog (2FGL, 2008 August 4 – 2010 August 4; Nolan et al. 2012), although a  $\gamma$ -ray source, 2FGL J2125.0–4632 with a radius of the 95% source location confidence region of  $0.17^\circ$ , at  $0.52^\circ$  from the radio position of PKS 2123–463 was reported. Taking into consideration the high variability of blazars, the flux of PKS 2123–463 could have decreased in the second year of *Fermi*-LAT operation. In addition, in the construction of the 2FGL catalog, PKS 2123–463 was split into more than one candidate source seed (see Section 4.2 of Nolan et al. 2012, for details). These two factors may have led to the lack of its association with a  $\gamma$ -ray source.

In this paper we present the localization over 41 months of *Fermi*-LAT data of a  $\gamma$ -ray source associated with the FSRQ PKS 2123–463. The correlated variability observed in optical, UV, X-ray and  $\gamma$  rays confirms the identification. In addition a new estimation of the redshift of the source by means of the fit of simultaneous GROND and *Swift*/UVOT data collected soon after the  $\gamma$ -ray flare is presented. The paper is organized as follows: in Section 2 we report the LAT data analyses and results. In Sections 3 and 4 we report the results of the *Swift* and GROND data analysis, respectively. Radio data collected by the ATCA, Ceduna and KAT-7 telescopes are presented in Section 5. Section 6 presents an estimation of the redshift of the source. In Section 7 we discuss the modeling of the overall SED and draw our conclusions. Throughout the paper a  $\Lambda$ -CDM cosmology with  $H_0 = 71$  km s $^{-1}$  Mpc $^{-1}$ ,  $\Omega_\Lambda = 0.73$ , and  $\Omega_m = 0.27$  is adopted.

## 2 FERMILAT DATA: SELECTION AND ANALYSIS

The *Fermi*-LAT is a  $\gamma$ -ray telescope operating from 20 MeV to  $> 300$  GeV. It has a large peak effective area ( $\sim 8000$  cm $^2$  for 1 GeV photons), an energy resolution of typically  $\sim 10\%$ , and a field of view of about 2.4 sr with an angular resolution (68% containment angle) better than  $1^\circ$  for energies above 1 GeV. Further details about the *Fermi*-LAT are given by Atwood et al. (2009).

The *Fermi*-LAT data reported in this paper were collected over the first 41 months of *Fermi* operation, from 2008 August 4 (MJD 54682) to 2012 January 4 (MJD 55930). During this time the LAT instrument operated almost entirely in survey mode. The spectral analysis was performed with the `ScienceTools` software package version v9r23p1. The *Fermi*-LAT data were extracted from a circular Region of Interest (RoI) with a  $15^\circ$  radius centred at the radio location of PKS 2123–463. Only events belonging to the ‘Source’ class were used. The time intervals when the rocking angle of the LAT was greater than  $52^\circ$  were rejected. In addition, a cut on the zenith angle ( $< 100^\circ$ ) was also applied to reduce contamination from the Earth limb  $\gamma$  rays, which are produced by cosmic rays interacting with the upper atmosphere. The spectral analyses (from which we derived spectral fits and photon fluxes) were performed with the post-launch instrument response functions (IRFs) `P7SOURCE_V6` using an unbinned maximum likelihood method implemented in the Science tool `glike`.

The background model used to extract the  $\gamma$ -ray signal includes a Galactic diffuse emission component and an isotropic component. The model that we adopted for the

<sup>1</sup> The corresponding luminosity distance for  $z = 1.46 \pm 0.05$  is  $d_L = 10.6 \pm 0.5$  Gpc and 1 arcsec corresponds to a projected distance of  $8.53 \pm 0.02$  kpc.

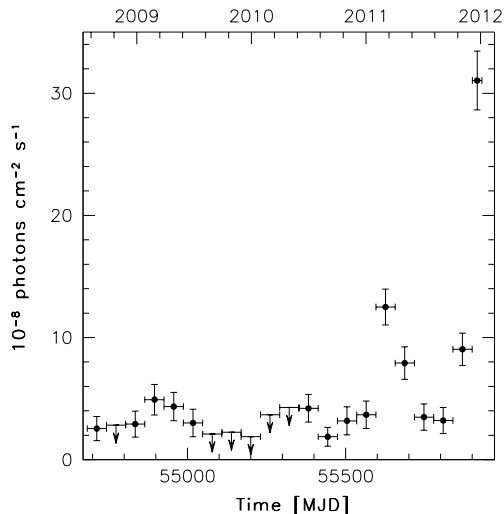


**Figure 1.** 2-month integrated flux ( $E > 100$  MeV) light curve of PKS 2123–463 obtained from 2008 August 4 to 2012 January 4 (MJD 54682–55930). The last bin covers 1 month of observation. Arrows refer to  $2\text{-}\sigma$  upper limits on the source flux. Upper limits are computed when  $\text{TS} < 10$ .

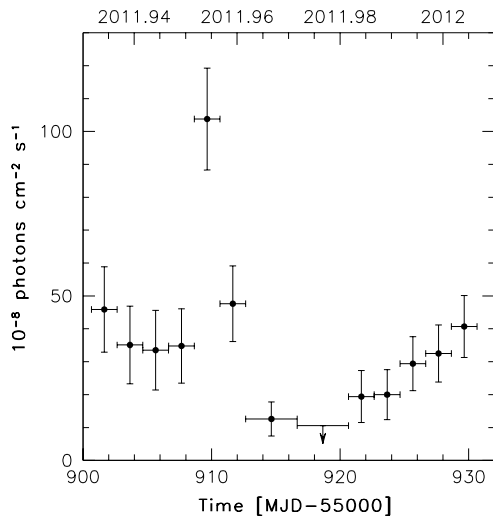


**Figure 2.** Integrated flux ( $E > 100$  MeV) light curve of PKS 2123–463 obtained from 2011 December 4 to 2012 January 4 (MJD 55899–55930) with 2-day or 4-day time bins. Arrows refer to  $2\text{-}\sigma$  upper limits on the source flux. Upper limits are computed when  $\text{TS} < 10$ .

Galactic component, the same as used for the 2FGL catalog, is given by the file `gal_2yearp7v6.v0.fits`, and the isotropic component, which is the sum of the extragalactic diffuse emission and the residual charged particle background, is parametrized by the file `iso_p7v6source.txt`<sup>2</sup>. The normalizations of both components in the background model were allowed to vary freely during the spectral point fitting.

We examine the significance of the  $\gamma$ -ray signal from

the sources using the Test Statistic (TS) based on the likelihood ratio test. The Test Statistic, defined as  $\text{TS} = 2\Delta\log(\text{likelihood})$  between models with and without the source, is a measure of the probability of having a  $\gamma$ -ray source at the localization specified, which compares models whose parameters have been adjusted to maximize the likelihood of the data given the model (Mattox et al. 1996). The source model used in `gtlike` includes all the point sources from the 2FGL that fall within  $20^\circ$  of PKS 2123–463. The spectra of those sources were parametrized by power-law functions, except for 2FGL J2056.2–4715 for which we used a log-parabola, and 2FGL J2124.6–3357 and 2FGL J2241.7–5236 for which we used an exponentially cut-off power-law in their spectral modeling as in the 2FGL catalog. We removed from the model the sources having  $\text{TS} < 25$  and/or fluxes (0.1–100 GeV) below  $1.0 \times 10^{-8}$  photons  $\text{cm}^{-2} \text{s}^{-1}$  over 41 months and repeated the fit. We tested whether two distinct  $\gamma$ -ray sources (one at the radio position of PKS 2123–463 and one at the  $\gamma$ -ray position of 2FGL J2125.0–4632) are detected simultaneously by *Fermi* with  $\text{TS} \geq 25$  over 41 months of observations. In this scenario, the fit yields a TS of 553 for PKS 2123–463 and a TS of 14 for 2FGL J2125.0–4632. We thus conclude that PKS 2123–463 and 2FGL J2125.0–4632 are the same source and we maintain only PKS 2123–463 in the model. Thus a final fitting procedure has been performed with all sources within  $10^\circ$  of PKS 2123–463 included with the normalization factors and the photon indices left as free parameters. For the sources located between  $10^\circ$  and  $15^\circ$  we kept the normalization and the photon index fixed to the values obtained in the previous fitting procedure. The RoI model includes also sources falling between  $15^\circ$  and  $20^\circ$  from the target source, which can contribute to the total counts observed in the RoI due to the energy-dependent size of the point spread function of the instrument. For these additional sources, normalizations and indices were fixed to the values of the 2FGL catalog during all steps of the fitting procedure.

The  $\gamma$ -ray point source localization using the `gtfindsrc` tool over the photons extracted during the period 2008 August 4 – 2012 January 4 results in R.A. =  $321.609^\circ$ , Dec. =  $-46.076^\circ$  (J2000), with a 95% error circle radius of  $0.047^\circ$ , at an angular separation of  $0.024^\circ$  from the radio position of PKS 2123–463 (R.A. =  $321.628^\circ$ , Dec. =  $-46.097^\circ$ , J2000). This implies a strict spatial association with PKS 2123–463. The fit with a power-law (PL) model,  $dN/dE \propto (E/E_0)^{-\Gamma}$ , to the data integrated over 41 months of *Fermi* operation in the 0.1–100 GeV energy range results in a  $\text{TS} = 557$ , with an integrated average flux of  $(4.76 \pm 0.35) \times 10^{-8}$  photons  $\text{cm}^{-2} \text{s}^{-1}$ , and a photon index  $\Gamma = 2.45 \pm 0.05$  (with  $E_0$  fixed to 670 MeV). In order to test for curvature in the  $\gamma$ -ray spectrum of PKS 2123–463 we used as an alternative spectral model the log-parabola (LP),  $dN/dE \propto (E/E_0)^{-\alpha-\beta \log(E/E_0)}$  (Landau et al. 1986; Massaro et al. 2004), where the parameter  $\alpha$  is the spectral slope at the energy  $E_0$  and the parameter  $\beta$  measures the curvature around the peak. We fixed the reference energy  $E_0$  to 300 MeV. The fit with a log-parabola results in a  $\text{TS} = 554$ , with spectral parameters  $\alpha = 2.35 \pm 0.09$ , and  $\beta = 0.06 \pm 0.04$ . Applying a likelihood ratio test to check the PL model (null hypothesis) against the LP model (alternative hypothesis), the power-law spectral model is favoured, indicating that no significant curvature was observed in the average  $\gamma$ -ray spectrum.

<sup>2</sup> <http://fermi.gsfc.nasa.gov/ssc/data/access/lat/BackgroundModels.html>

Figure 1 shows the  $\gamma$ -ray light curve of the first 41 months of *Fermi* observations of PKS 2123–463 built using 2-month time bins, with the exception of the final (1-month) data point. For each time bin the photon index was frozen to the value resulting from the likelihood analysis over the entire period. If  $TS < 10$  2- $\sigma$  upper limits were calculated instead. The systematic uncertainty in the flux is energy dependent: it amounts to 10% at 100 MeV, decreasing to 5% at 560 MeV, and increasing to 10% above 10 GeV (Ackermann et al. 2012).

As shown in Fig. 1 PKS 2123–463 was in a low  $\gamma$ -ray state (0.1–100 GeV flux  $< 5 \times 10^{-8}$  ph cm $^{-2}$  s $^{-1}$ ) for the first 2.5 years. In particular the source was not detected with 2-month time bin during the period 2009 August–2010 May. A first increase of the  $\gamma$ -ray flux was observed in 2011 February–March, and subsequently a flaring activity in 2011 December. We show a light curve focused on the period of high activity (2011 December 4–2012 January 4; MJD 55899–55930) with 2-day or 4-day time bins (Fig. 2). The peak of the emission was observed between December 13 15:43 UT and December 14 15:43 UT, with a flux of  $(128 \pm 23) \times 10^{-8}$  photons cm $^{-2}$  s $^{-1}$  in the 0.1–100 GeV energy range, a factor of  $\sim 25$  higher with respect to the average  $\gamma$ -ray flux observed during 2008–2011. The corresponding observed isotropic  $\gamma$ -ray luminosity peak in the 0.1–100 GeV energy range is  $8.9 \pm 0.8 \times 10^{48}$  erg s $^{-1}$  (assuming  $z = 1.46 \pm 0.05$ , see Sect. 6), comparable to the values reached by the most powerful FSRQs in flaring activity (e.g. Orienti et al. 2012; Ackermann et al. 2010). Leaving the photon index free to vary during the period of high activity and  $E_0$  fixed to 670 MeV the fit results in a photon index  $\Gamma = 2.26 \pm 0.06$ , showing a moderate harder-when-brighter behaviour already observed in other FSRQs (Abdo et al. 2010b). Replacing in the same period the PL with a LP, fixing the reference energy  $E_0$  to 300 MeV, we obtain spectral parameters  $\alpha = 2.09 \pm 0.13$ , and  $\beta = 0.10 \pm 0.04$ . We used a likelihood ratio test to check the PL model (null hypothesis) against the LP model (alternative hypothesis). These values may be compared, following Nolan et al. (2012), by evaluating the curvature Test Statistic  $TS_{curve} = 2(\log(\text{like})_{LP} - \log(\text{like})_{PL}) = 3$  ( $\sim 1.7\text{-}\sigma$ ); thus no significant curvature was observed in the  $\gamma$ -ray spectrum also during the high activity period.

Finally, using the `gtsrcprob` tool, which calculates the probabilities an event belongs to each of the sources in the model, we estimated that the highest-energy photon emitted by PKS 2123–463 was observed with a probability of 87% at distance of  $0.35^\circ$  from the source with an energy of 92 GeV. For a single high-energy photon ( $\geq 1$  GeV), sky location can only be determined within  $\sim 0.8^\circ$  (95% confidence radius).

### 3 SWIFT DATA: ANALYSIS AND RESULTS

The *Swift* satellite (Gehrels et al. 2004) performed two observations of PKS 2123–463 in 2011 December triggered by the  $\gamma$ -ray flare detected by *Fermi*-LAT. As a comparison we also analysed two additional observations performed during 2010–2011. The observations were performed with all three on-board instruments: the X-ray Telescope (XRT; Burrows et al. 2005, 0.2–10.0 keV), the UltraViolet Optical Telescope (UVOT; Roming et al. 2005, 170–600 nm) and the

Burst Alert Telescope (BAT; Barthelmy et al. 2005, 15–150 keV).

The hard X-ray flux of this source is below the sensitivity of the BAT instrument for the short exposure time of these observations. Moreover, the source was not present in the *Swift* BAT 58-month hard X-ray catalog (Baumgartner et al. 2010) and the 54-month Palermo BAT catalog (Cusumano et al. 2010).

#### 3.1 Swift/XRT

The XRT data were processed with standard procedures (`xrtpipeline v0.12.6`), filtering, and screening criteria by using the `HEASOFT` package (v6.11)<sup>3</sup>. The data were collected in photon counting mode in all observations, and only XRT event grades 0–12 were selected. The source count rate was low ( $< 0.5$  cnt s $^{-1}$ ); thus pile-up correction was not required. Source events were extracted from a circular region with a radius of 20 pixels (1 pixel  $\sim 2''.36$ ), while background events were extracted from a circular region with a radius of 50 pixels away from the source region. Ancillary response files were generated with `xrtmkarf`, and account for different extraction regions, vignetting and point spread function (PSF) corrections. We used the spectral redistribution matrices v013 in the Calibration database maintained by HEASARC.

Considering the low number of photons collected ( $< 200$  counts) the spectra were rebinned with a minimum of 1 count per bin and the Cash statistic (Cash 1979) was applied. We fitted the spectrum with an absorbed power-law using the photoelectric absorption model `tbabs` (Wilms et al. 2000), with a neutral hydrogen column fixed to its Galactic value ( $2.34 \times 10^{20}$  cm $^{-2}$ ; Kalberla et al. 2005). The fit results are reported in Table 1 and Fig. 4.

A marginal increase (1.5  $\sigma$ ) of the X-ray flux with respect to the previous *Swift*/XRT observations was observed on 2011 December 15, soon after the  $\gamma$ -ray flare. The source remained at a similar flux level in X-rays on 2011 December 19.

#### 3.2 Swift/UVOT

UVOT UV/optical imaging was obtained during all four *Swift* observations of PKS 2123–463. The photometry was carried out on pipeline processed sky images downloaded from the *Swift* data center<sup>4</sup>, following the standard UVOT procedure (Poole et al. 2008). Source photometric measurements were extracted from the UVOT imaging data using the tool `UVOTMAGHIST` (v1.1) with a circular source extraction region that ranged from  $3''.5$ – $5''$  radius to maximize the signal-to-noise. In order to remain compatible with the effective area calibrations, which are based on  $5''$  aperture photometry (Poole et al. 2008), an aperture correction was applied where necessary. This correction was at maximum 5–6% of the flux, depending on the filter. The UVOT photometry is presented in Table 2 and Fig. 4. Contemporaneous UVOT observations in 2011 December 15 found PKS 2123–463 about 0.5 mag brighter in  $v$ -,  $u$ -, and  $w$ 1-band, 0.7

<sup>3</sup> <http://heasarc.nasa.gov/lheasoft/>

<sup>4</sup> <http://www.swift.ac.uk/swift-portal>

**Table 1.** Log and fitting results of *Swift*/XRT observations of PKS 2123–463 using a power-law model with  $N_{\text{H}}$  fixed to Galactic absorption.

MJD	UT Date	Exposure Time [sec]	$\Gamma$	Flux (0.3–10 keV) <sup>a</sup> [ $\times 10^{-12}$ erg cm <sup>-2</sup> s <sup>-1</sup> ]
55467	2010-09-28	2712	1.47 $\pm$ 0.30	1.31 $\pm$ 0.46
55745	2011-07-03	2912	1.61 $\pm$ 0.28	1.20 $\pm$ 0.32
55910	2011-12-15	4947	1.68 $\pm$ 0.18	1.90 $\pm$ 0.34
55914	2011-12-19	5521	1.26 $\pm$ 0.18	1.83 $\pm$ 0.27

<sup>a</sup>: Observed flux.

**Table 2.** UVOT Photometry of PKS 2123–463.

UT Date	AB Magnitude <sup>a</sup>					
	<i>uvw2</i>	<i>uvm2</i>	<i>uvw1</i>	<i>u</i>	<i>b</i>	<i>v</i>
2010-09-28 18:29-23:30	19.78 $\pm$ 0.09	19.34 $\pm$ 0.10	19.17 $\pm$ 0.10	18.66 $\pm$ 0.09	18.61 $\pm$ 0.14	18.59 $\pm$ 0.20
2011-07-03 17:15-23:29	19.83 $\pm$ 0.20	19.28 $\pm$ 0.14	18.75 $\pm$ 0.11	18.47 $\pm$ 0.12	18.81 $\pm$ 0.25	18.21 $\pm$ 0.26
2011-12-15 20:45-01:25	18.97 $\pm$ 0.06	18.58 $\pm$ 0.06	18.24 $\pm$ 0.05	17.95 $\pm$ 0.06	-	17.64 $\pm$ 0.06
2011-12-19 04:20-04:39	19.17 $\pm$ 0.12	18.80 $\pm$ 0.12	18.51 $\pm$ 0.09	18.04 $\pm$ 0.07	17.77 $\pm$ 0.07	17.82 $\pm$ 0.15

<sup>a</sup>: Corrected for Galactic foreground reddening of  $E_{\text{B}-\text{V}} = 0.03$  mag (Schlegel et al. 1998).

mag in *m2*-band, and about 0.8 mag in *w2*-band compared to the UVOT observation performed on 2011 July 3.

#### 4 GROND DATA

On 2011 December 18, at 01:21 UT, PKS 2123–463 was observed with the Gamma-ray Optical/Near-Infrared Detector (GROND; Greiner et al. 2008) mounted on the MPG/ESO 2.2-m telescope at La Silla, Chile. Preliminary results have been reported in Rau et al. (2011). GROND is a 7-channel imager that observes in four optical and three near-IR channels simultaneously. The data were reduced and analysed with the standard tools and methods described in Krühler et al. (2008). Calibration was performed against an SDSS standard star field ( $g'r'i'z'$ ) and against selected 2MASS stars (Skrutskie et al. 2006) ( $JHK_S$ ). This resulted in 1- $\sigma$  accuracies of 0.05 mag ( $g'r'i'z'$ , J, H), and 0.07 mag ( $K_S$ ). All magnitudes are corrected for Galactic foreground extinction of  $E_{\text{B}-\text{V}} = 0.030$  mag (Schlegel et al. 1998) and are summarised in Table 3.

#### 5 RADIO DATA

PKS 2123–463 is monitored by the TANAMI program (Tracking Active galactic Nuclei with Austral Milliarcsecond Interferometry; Ojha et al. 2010) at a number of radio frequencies and resolutions with the Australia Telescope Compact Array (ATCA) and the Ceduna facilities. ATCA is observing this source every few weeks with “snapshot” observations at frequencies from 5.5 GHz through 40 GHz where each frequency is the centre of a 2 GHz wide band and the fluxes are calibrated against the ATCA primary flux calibrator PKS 1934–638 (Stevens et al. 2012). Each flux density has a 1- $\sigma$  uncertainty of 0.01 Jy. The Ceduna radio telescope in South Australia is monitoring PKS 2123–463 at 6.7 GHz. Each flux density has a 1- $\sigma$  uncertainty of 0.3 Jy (McCulloch et al. 2005). No sign of increased activity of the

**Table 4.** ATCA (5.5, 9, 17, 19, 38, and 40 GHz) and Ceduna (6.7 GHz) observations of PKS 2123–463 in 2011.

UT Date	Frequency (GHz)	Flux (Jy)
2011-05-17	5.5	0.86
	9.0	0.77
	17.0	0.67
	19.0	0.64
	38.0	0.45
	40.0	0.44
2011-10-14	5.5	0.86
	9.0	0.76
	17.0	0.60
	19.0	0.56
	38.0	0.42
	40.0	0.41
2011-11-08	5.5	0.85
	9.0	0.71
	17.0	0.57
	19.0	0.53
	38.0	0.43
	40.0	0.43
2011-12-19	6.7	0.81
2012-02-18	6.7	0.78

flux density was detected between 40 and 5.5 GHz before the  $\gamma$ -ray flare (see Fig. 4).

In addition observations of PKS 2123–463 were made after the  $\gamma$ -ray outburst using the KAT-7 array (the prototype for MeerKAT) in the Karoo. Since the array is still undergoing commissioning tests some uncertainties remained about the absolute calibration scale. To minimize these uncertainties the observations were taken at similar times of days (hence Local Sidereal Time range) in late 2011 December to early 2012 January, with 4–5 hr durations. The very first observation (December 21) failed because the online

**Table 3.** GROND Photometry of PKS 2123–463.

UT Date	$g'$	$r'$	$i'$	AB Magnitude <sup>a</sup> $z'$	$J$	$H$	$K_s$
2011-12-18 01:21	$17.78 \pm 0.05$	$17.52 \pm 0.05$	$17.43 \pm 0.05$	$17.24 \pm 0.05$	$16.75 \pm 0.06$	$16.53 \pm 0.06$	$16.24 \pm 0.09$

<sup>a</sup>: Corrected for Galactic foreground reddening of  $E_{B-V} = 0.03$  mag (Schlegel et al. 1998).

fringe stopping was not working properly, but as the array is very small (longest baseline 200-m) and the frequency low enough (1.822 GHz) the delay tracking corrections could be done offline with only marginal loss in signal to noise ratio. Subsequent observations were done in this mode. There were also different problems with various receivers over this time so  $uv$ -coverage and maps were not directly comparable. The bandpass and gain solutions (on PKS 1934–638) were good enough and checks against a nearby phase reference source (PKS 2134–470) gave sufficient confidence in the visibilities and phases to make simple maps of the inner  $0.5^\circ$  of the primary beam and verify that no sources stronger than 100 mJy were present.

Assuming a flux density for PKS 1934–638 of 13.6 Jy at 1.822 GHz (as interpolated from ATCA models) the measured flux density of PKS 2123–463 is 1.13 Jy on 2011 December 24, 26, 29, and 2012 January 7 and 13. The uncertainties on the absolute flux density scale is 5%. As a comparison we extrapolate the flux density at 1.82 GHz using the values at 2.7, 0.8, and 0.4 GHz from the Parkes Catalogue (1990) and the Molonglo Sky Survey (2008). Assuming the spectral index 0.4 derived between 2.7 and 0.4 GHz, we obtain a flux density at 1.82 GHz of 1.0 Jy, indicating that no significant variation was observed during the  $\gamma$ -ray flaring activity at this frequency.

## 6 NEW PHOTOMETRIC REDSHIFT ESTIMATION

The redshift of PKS 2123–463 has not been established convincingly yet. Following the method described in Rau et al. (2012) and applied to a sample of 103 *Fermi*-LAT blazars, we combined the GROND photometry with the UVOT photometry from 2011 December 19 in order to construct a 13-band spectral energy distribution (SED). In order to account for source-intrinsic variability between the GROND and UVOT observing epochs, the GROND photometry was corrected by  $-0.05$  mag in all bands (see Rau et al. 2012, for a detailed description of the method). The resulting SED, corrected for the Galactic foreground reddening of  $E_{B-V} = 0.03$  mag (Schlegel et al. 1998), has been fit with a set of power-law models as well as with hybrid templates built from normal galaxies and AGN (Salvato et al. 2009, 2011) using the Le PHARE code (Arnouts et al. 1999; Ilbert et al. 2006). The best-fitting redshifts for both template libraries are in good agreement (see Fig. 3). For the power-law model we obtain a 99% confidence redshift of  $z = 1.37_{-0.21}^{+0.13}$  ( $\chi^2 = 17$ ,  $P_z = 94.6$ <sup>5</sup>) and for the hybrid

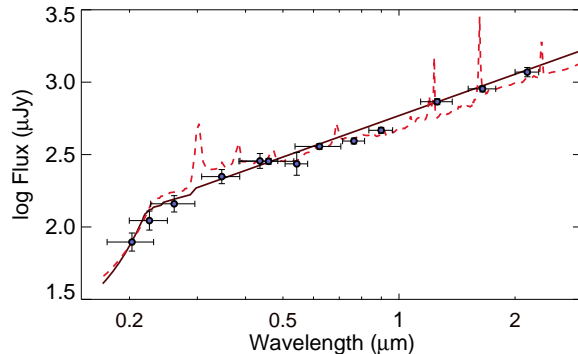


**Figure 3.** UV-near-IR SED composed of *Swift*/UVOT observations obtained on 2011 December 19 and GROND data taken on 2011 December 18. The simple power-law model (solid line) and the AGN/galaxy hybrid template (dashed line) suggest a photometric redshift of  $z \approx 1.45$  (see text for details).

models we find  $z = 1.46 \pm 0.05$  ( $\chi^2 = 23$ ,  $P_z = 99.2$ ). This is in rough agreement with the initial spectroscopic redshift of  $z = 1.67$  from Savage & Wright (1981).

## 7 SED MODELING AND CONCLUSIONS

Beyond the excellent spatial association obtained with the 41-month *Fermi*-LAT data set, the most secure and distinctive signature for firm identification of the  $\gamma$ -ray source detected by *Fermi*-LAT with the blazar PKS 2123–463 is the simultaneous increase observed in the  $\gamma$ -ray, X-ray, and optical-UV bands (see Fig. 4, Sections 2 and 3).

In order to investigate the physical properties of the source we have built a simultaneous SED of the flaring state of PKS 2123–463. The *Fermi*-LAT spectrum was built with data from observations centred on 2011 December 10 to 19 (MJD 55905–55916). In addition we included in the SED the GROND and *Swift* (UVOT and XRT) data collected on 2011 December 18 and December 19, respectively. Here, the flux suppression, in particular in the UV bands, was corrected assuming a power-law spectral shape consistent with the optical-near-IR measurements ( $F_\lambda \propto \lambda^{0.8}$ ). The data from ATCA and KAT-7 collected on December 19 and 24, respectively, provided information about the radio part of the spectrum. The flare centred on  $\sim$  MJD 55909 had a variability timescale of  $\sim 2$  days, which constrains the size of the emitting region during the flare to  $R'_b \lesssim 2.1 \times 10^{16} (\delta_D/20)$  cm.

<sup>5</sup> The best fit templates and redshifts were selected on the basis of a simple  $\chi^2$  method.  $P_z$  is the integral of the probability distribution function  $\int f(z)dz$  at  $z_{\text{phot}} \pm 0.1(1 + z_{\text{phot}})$ , which

describes the probability that the redshift of a source is within  $0.1(1 + z)$  of the best fit value.

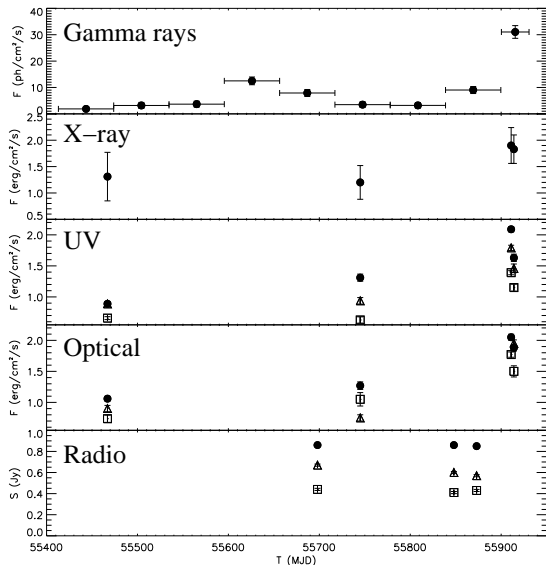


**Figure 4.** Light curves of PKS 2123–463 collected in  $\gamma$  rays by *Fermi*-LAT (0.1–100 GeV flux in units of  $10^{-8}$  ph  $\text{cm}^{-2}$   $\text{s}^{-1}$ ), in X-rays by *Swift*/XRT (flux in units of  $10^{12}$  erg  $\text{cm}^{-2}$   $\text{s}^{-1}$ ), in UV (filters w1: empty squares, m2: empty triangles, w2: filled circles; flux in units of  $10^{12}$  erg  $\text{cm}^{-2}$   $\text{s}^{-1}$ ), and in optical (filters u: empty squares, b: empty triangles, v: filled circles; flux in units of  $10^{13}$  erg  $\text{cm}^{-2}$   $\text{s}^{-1}$ ) by *Swift*/UVOT, and radio by ATCA (empty squares: 40 GHz, empty triangles: 17 GHz, filled circle: 5.5 GHz) between 2010 June and 2011 December.

A “blue bump” accretion disc component is clearly visible in the optical/UV data. We modeled these data with a combination of a nonthermal synchrotron component and a Shakura-Sunyaev disc component (Shakura and Sunyaev 1973). A fit to the disc component allows us to get a rough estimate of the black hole mass of  $M_{BH} \approx 2 \times 10^9 M_{\odot}$ . This is the first black hole mass estimate for this source. It is consistent with black hole estimates for other high- $z$  FSRQs, obtained in a similar way by Ghisellini et al. (2011). Our mass estimate for PKS 2123–463 follows Ghisellini et al. (2011) and assumes that the innermost stable circular orbit (ISCO) is  $R_{disc,ISCO} = 6R_g$ , as one would expect for a Schwarzschild (i.e., nonrotating) black hole. If the jet is produced by the Blandford-Znajek (Blandford & Znajek 1977) or Blandford-Payne (Blandford & Payne 1982) mechanisms this requires a nonzero black hole spin, and one expects  $R_{disc,ISCO}$  to be smaller or larger, depending on whether the spin is retrograde or prograde (e.g., Garofalo et al. 2010). Due to the uncertainty in spin, this mass estimate can be considered to have considerable uncertainty.

We modelled the portion of the SED from X-rays to  $\gamma$  rays assuming emission from a relativistic jet with mechanisms of synchrotron self-Compton (SSC), and Compton-scattering of a dust torus external to the jet (EC-dust). The description of the model can be found in Finke et al. (2008) and Dermer et al. (2009). The synchrotron component considered is self-absorbed below  $\sim 10^{11}$  Hz. Correlations of  $\gamma$ -ray and optical flares with radio light curves and rotations of optical polarisation angles in low-synchrotron-peaked blazars seem to indicate the  $\gamma$ -ray/optical emitting region is outside the broad line region (BLR), where the dust

torus is the likely seed photon source (e.g., Marscher et al. 2010). From the disc luminosity obtained by the fit of the blue bump,  $L_{disc} = 1.8 \times 10^{46}$  erg  $\text{s}^{-1}$ , we estimate an associated BLR radius  $R_{BLR} = 4.4 \times 10^{17}$  cm, based on the relation between disc luminosity and  $R_{BLR}$  determined from reverberation mapping campaigns (e.g., Kaspi et al. 2005; Ghisellini et al. 2008). To minimize the scattered BLR contribution, we placed the emitting region at  $r > R_{BLR}$ . Here the primary seed photon source is the dust torus, which was simulated as a one-dimensional ring with radius  $R_{dust}$  aligned orthogonal to the jet, emitting as a blackbody with temperature  $T_{dust}$  and luminosity  $L_{dust}$ .

The model fit to the broadband SED can be seen in Fig. 5 and the parameters can be found in Table 5. A description of the parameters can be found in Dermer et al. (2009). The dust parameters were chosen so that  $R_{dust}$  is roughly consistent with the sublimation radius (Nenkova et al. 2008). The EC-BLR component was calculated assuming the seed photons are from H $\alpha$  and have a luminosity of  $0.1L_{disc}$ .

The electron distribution used, a broken power-law with index  $p_1 = 2.0$  below the break at  $\gamma'_{brk}$  and  $p_2 = 3.8$  for  $\gamma'_{brk} < \gamma'$ , is consistent with particles injected with index 2.8, and emission taking place in the *fast cooling regime* (e.g., Böttcher & Dermer 2002). That is, particles are injected between  $\gamma'_{brk}$  and  $\gamma'_{max}$ , with a cooling electron Lorentz factor

$$\gamma_{cool} \equiv \frac{3m_e c^2}{4\sigma_T t_{esc} u_{tot}}$$

where  $u_{tot}$  is the total energy density in the blob frame, which in the case of our model fit is dominated by the external energy density. In this case  $\gamma_{cool}$  is associated with  $\gamma_{min}$ , since it is in the fast cooling regime. Also note that in this model fit the magnetic field and electrons are nearly in equipartition. Jet powers were calculated assuming a two-sided jet.

The Compton dominance for PKS 2123–463, i.e., the ratio of the peak luminosities of the Compton and synchrotron components, is  $\approx 50$ , which is a rather standard value for powerful blazars (e.g., Ghisellini et al. 2011). A large disc luminosity was estimated from the UVOT data, as expected for a powerful FSRQ, with a  $L_{disc}/L_{Edd} = 0.2$  in agreement with the blazar divide proposed by Ghisellini et al. (2009) as a result of the changing of the accretion mode.

Variability is common in  $\gamma$ -ray blazars and provides a powerful tool to associate them definitively with objects known at other wavelengths and to study the emission mechanisms at work. The combination of deep and fairly uniform exposure over  $\sim 3$  hr, very good angular resolution, and stable response of the *Fermi*-LAT is producing the most sensitive, best-resolved survey of the  $\gamma$ -ray sky. On the other hand, those cases where there is a decrease in the activity, and thus of the significance of detection, can lead to a more complex identification process for a  $\gamma$ -ray source. When combined with simultaneous ground- and space-based multifrequency observations, the *Fermi*-LAT achieves its full capability for the identification of the  $\gamma$ -ray sources with counterparts at lower energies and the knowledge of their emission processes, as reported here for the high- $z$ , Compton-dominated FSRQ PKS 2123–463.

**Table 5.** Model parameters for the SED shown in Fig. 5.

Redshift	$z$	1.46
Bulk Lorentz Factor	$\Gamma$	20
Doppler Factor	$\delta_D$	20
Magnetic Field	$B$	0.8 G
Variability Timescale	$t_v$	$1.7 \times 10^5$ s
Comoving radius of blob	$R'_b$	$4.1 \times 10^{16}$ cm
Jet Height	$r$	$1.0 \times 10^{18}$ cm
Low-Energy Electron Spectral Index	$p_1$	2.0
High-Energy Electron Spectral Index	$p_2$	3.8
Minimum Electron Lorentz Factor	$\gamma'_{min}$	4.0
Break Electron Lorentz Factor	$\gamma'_{brk}$	$1.0 \times 10^3$
Maximum Electron Lorentz Factor	$\gamma'_{max}$	$1.0 \times 10^5$
Disc Luminosity	$L_{disc}$	$1.8 \times 10^{46}$ erg s $^{-1}$
Black Hole Mass	$M_{BH}$	$2 \times 10^9 M_\odot$
Accretion efficiency	$\eta$	1/12
Gravitational Radius	$R_g$	$1.76 \times 10^{14}$ cm
Inner Disc Radius	$R_{disc-ISCO}$	6 $R_g$
Outer Disc Radius	$R_{disc-max}$	$10^4 R_g$
Dust Torus luminosity	$L_{dust}$	$1.5 \times 10^{45}$ erg s $^{-1}$
Dust Torus temperature	$T_{dust}$	$1.7 \times 10^3$ K
Dust Torus radius	$R_{dust}$	$3.2 \times 10^{18}$ cm
Jet Power in Magnetic Field	$P_{j,B}$	$3.3 \times 10^{45}$ erg s $^{-1}$
Jet Power in Electrons	$P_{j,par}$	$1.5 \times 10^{45}$ erg s $^{-1}$

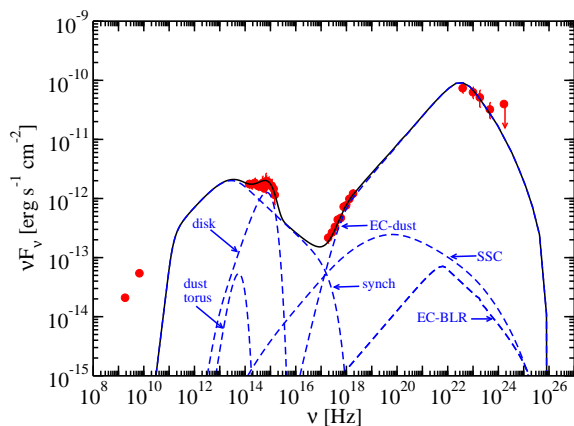


**Figure 5.** Spectral energy distribution data (circles and squares) and model fit (solid curve) of PKS 2123–463 with the model components shown as dashed curves. The data points were collected by GROND (2011 December 18), *Swift* (UVOT and XRT; 2011 December 19), and *Fermi*-LAT (2011 December 10-19), together with radio data from ATCA (2011 December 19) and KAT-7 (2011 December 24).

## ACKNOWLEDGMENTS

The *Fermi* LAT Collaboration acknowledges generous ongoing support from a number of agencies and institutes that have supported both the development and the operation of the LAT as well as scientific data analysis. These include the National Aeronautics and Space Administration and the Department of Energy in the United States, the Commissariat à l’Energie Atomique and the Centre National de la Recherche Scientifique / Institut National de Physique Nucléaire et de Physique des Particules in France, the Agenzia Spaziale Italiana and the Istituto Nazionale di Fisica Nu-

cleare in Italy, the Ministry of Education, Culture, Sports, Science and Technology (MEXT), High Energy Accelerator Research Organization (KEK) and Japan Aerospace Exploration Agency (JAXA) in Japan, and the K. A. Wallenberg Foundation, the Swedish Research Council and the Swedish National Space Board in Sweden. Additional support for science analysis during the operations phase is gratefully acknowledged from the Istituto Nazionale di Astrofisica in Italy and the Centre National d’Études Spatiales in France.

Part of the funding for GROND (both hardware as well as personnel) was generously granted from the Leibniz-Prize to Prof. G. Hasinger (DFG grant HA 1850/28-1). We thank the *Swift* team for making these observations possible, the duty scientists, and science planners. DAK acknowledges support by DFG grant Kl 766/16-1, and is grateful for travel funding support through MPE. The Australia Telescope Compact Array is part of the Australia Telescope National Facility which is funded by the Commonwealth of Australia for operation as a National Facility managed by CSIRO. This research was funded in part by NASA through Fermi Guest Investigator grant NNH09ZDA001N (proposal number 31263). This research was supported by an appointment to the NASA Postdoctoral Program at the Goddard Space Flight Center, administered by Oak Ridge Associated Universities through a contract with NASA. We thank Silvia Rainó and the anonymous referee for useful comments and suggestions.

## REFERENCES

- Abdo, A. A., et al. 2010a, *ApJS*, 188, 405
- Abdo, A. A., et al. 2010b, *ApJ*, 710, 1271
- Ackermann, M., et al. 2010, *ApJ*, 721, 1383
- Ackermann, M., et al. 2012, accepted for publication in *ApJS* [arXiv:1206.1896]



- Arnouts, S., Cristiani, S., Moscardini, L., Matarrese, S., Lucchin, F., Fontana, A., Giallongo, E. 1999, *MNRAS*, 310, 540
- Atwood, W. B., et al. 2009, *ApJ*, 697, 1071
- Barthelmy, S. D., et al. 2005, *SSRv*, 120, 143
- Baumgartner, W. H., Tueller, J., Markwardt, C., Skinner, G. 2010, *HEAD*, 11, 130
- Blandford, R. D., & Znajek, R. L. 1977, *MNRAS*, 179, 433
- Blandford, R. D., & Rees, M. 1978, *Proceedings of Pittsburgh Conference on BL Lac Objects*. Pittsburgh Press, ed. Wolfe, A.M., pp. 328347
- Blandford, R. D., & Payne, D. G. 1982, *MNRAS*, 199, 883
- Böttcher, M., & Dermer, C. D. 2002, *ApJ*, 564, 86
- Burrows, D. N., et al. 2005, *SSRv*, 120,165
- Cash, W. 1979, *ApJ*, 228, 939
- Cusumano, G., et al. 2010, *A&A*, 524, 64
- D’Ammando, F., Orienti, M., Mountford, C. J. 2011, *The Astronomer’s Telegram* 3815
- Dermer, C. D., Finke, J. D., Krug, H., Böttcher, M. 2009, *ApJ*, 692, 32
- Fey, A. L., et al. 2006, *AJ*, 132, 1944
- Finke, J. D., Dermer, C. D., Böttcher, M. 2008, *ApJ*, 686, 181
- Garofalo, D., Evans, D. A., Sambruna, R. M. 2010, *MNRAS*, 406, 975
- Gehrels, N., et al. 2004, *ApJ*, 611, 1005
- Ghisellini, G., & Tavecchio, F. 2008, *MNRAS*, 387, 1669
- Ghisellini, G., Foschini, L., Volonteri, M., Ghirlanda, G., Haardt, F., Burlon, D., Tavecchio, F. 2009, *MNRAS*, 399, 2041
- Ghisellini, G., et al. 2011, *MNRAS*, 411, 901
- Greiner, J., Bornemann, W., Clemens, C., et al. 2008, *PASP*, 120, 405
- Healey, S., Romani, R. W., Taylor, G. B., Sadler, E. M., Ricci, R., Murphy, T., Ulvestad, J. S., Winn, J. N. 2007, *ApJS*, 171, 61
- Healey, S., et al. 2008, *ApJS*, 175, 97
- Ilbert, O., et al. 2006, *A&A*, 457, 841
- Jackson, C. A., Wall, J. V., Shaver, P. A., Kellermann, K. I., Hook, I. M., Hawkins, M. R. S. 2002, *A&A*, 386, 97
- Kalberla, P. M. W., Burton, W. B., Hartmann, Dap, Arnal, E. M., Bajaja, E., Morras, R., Pöppel, W. G. L. 2005, *A&A*, 440, 775
- Kaspi, S., Maoz, D., Netzer, H., Peterson, B. M., Vestergaard, M., Jannuzi, B. T. 2005, *ApJ*, 629, 61
- Krüehler, T., Küpcü Yoldaş, A., Greiner, J., et al. 2008, *ApJ*, 685, 376
- Landau, R., et al. 1986, *ApJ*, 308, 78
- Marscher, A. P., Jorstad, S. G., Larionov, V. M., et al. 2010, *ApJ*, 710, L126
- Marshall, H. L., Gelbord, J. M., Schwartz, D. A., et al. 2011, *ApJS*, 193, 15
- Massardi, M., et al. 2008, *MNRAS*, 384, 775
- Massaro, E., Perri, M., Giommi, P., Nesci, R. 2004, *A&A*, 413, 489
- Massaro, E., Giommi, P., Leto, C., Marchegiani, P., Maselli, A., Perri, M., Piranomonte, S., Sclavi, S. 2009, *A&A*, 495, 691
- Matttox, J. R., et al. 1996, *ApJ*, 461, 396
- McCulloch, P. M., Ellingsen, S. P., Jauncey, D. L., Carter, S. J. B., Cim, G., Lovell, J. E. J., Dodson, R. G. 2005, *AJ*, 129, 2034
- Nenkova, M., Sirocky, M. M., Nikutta, R., Ivezić, Ž., & Elitzur, M. 2008, *ApJ*, 685, 160
- Nolan, P. L., et al. 2012, *ApJS*, 199, 31
- Ojha, R., et al. 2010, *A&A*, 519, 45
- Orienti, M., & D’Ammando, F. 2011, *The Astronomer’s Telegram* 3808
- Orienti, M., Koyama, S., D’Ammando, F., et al. 2012, submitted to *MNRAS*
- Poole, T. S., Breeveld, A. A., Page, M. J., et al. 2008, *MNRAS*, 383, 627
- Rau, A., Schady, P., Greiner, J., Kann, D. A. 2011, *The Astronomer’s Telegram* 3814
- Rau, A., Schady, P., Greiner, J., Salvato, M., Ajello, M. et al. 2012, *A&A*, 538, A26
- Roming, P. W. A., et al. 2005, *SSRv*, 120, 95
- Salvato, M., et al. 2009, *ApJ*, 690, 1250
- Salvato, M., et al. 2011, *ApJ*, 742, 61
- Savage, A. & Wright, A. E. 1981, *MNRAS*, 196, 927
- Schlegel, D. J., Finkbeiner, D. P., Davis, M., *ApJ* 500, 525
- Shakura, N. I., & Sunyaev, R. A. 1973, *A&A*, 24, 337
- Skrutskie, M. F., Cutri, R. M., Stiening, R., et al. 2006, *AJ*, 131, 1163
- Stevens, J. A., et al. 2012, *Proceedings of Fermi & Jansky: Our Evolving Understanding of AGN*, St Michaels, MD, November 10-12, 2011, edited by R. Ojha, D. J. Thompson and C. Dermer, eConf C1111101, arXiv:1205.2403
- Urry, C. M., & Padovani, P. 1995, *PASP* 107, 803
- Wilms, J., Allen, A., McCray, R. 2000, *ApJ*, 542, 914